HHS Public Access

Author manuscript

Cell Stem Cell. Author manuscript; available in PMC 2018 April 29.

Published in final edited form as:

Cell Stem Cell. 2016 September 01; 19(3): 326–340. doi:10.1016/j.stem.2016.07.002.

An isogenic hESC platform for functional evaluation of GWAS-identified diabetes genes and drug discovery

Hui Zeng[1,2,Δ], **Min Guo**[2,5,Δ], **Ting Zhou**[2], **Lei Tan**[2], **Chi Nok Chong**[2], **Tuo Zhang**[4], **Xue Dong**[2], **Jenny Zhaoying Xiang**[4], **Albert S. Yu**[6], **Lixia Yue**[6], **Qibin Qi**[7], **Todd Evans**[2], **Johannes Graumann**[3,8], and **Shuibing Chen**[2,3,*]

[1]Department of Hematology, Central South University, 87 Xiangya Rd, Changsha, Hunan, China

[2]Department of Surgery, Weill Cornell Medical College, 1300 York Ave, New York, NY, USA

[3]Department of Biochemistry, Weill Cornell Medical College, 1300 York Ave, New York, NY, USA

[4]Genomic Core, Weill Cornell Medical College, 1300 York Ave, New York, NY, USA

[5]Department of Endocrinology in Xiangya hospital, Central South University, 87 Xiangya Rd, Changsha, Hunan, China

[6]Calhoun Cardiology Center, Department of Cell Biology, University of Connecticut Health Center, 263 Farmington Ave, Farmington, USA

[7]Department of Epidemiology and Population Health, Albert Einstein College of Medicine, 1300 Morris Park Avenue, Bronx, NY, USA

[8]Research Division, Weill Cornell Medical College in Qatar, Doha, State of Qatar

SUMMARY

Genome wide association studies (GWAS) have increased our knowledge of loci associated with a range of human diseases. However, applying such findings to elucidate pathophysiology and promote drug discovery remains challenging. Here, we created isogenic human embryonic stem cells (hESCs) with mutations in GWAS-identified susceptibility genes for type 2 diabetes. In pancreatic betalike cells differentiated from these lines, we found that mutations in CDKAL1, KCNQ1 and KCNJ11 led to impaired glucose secretion in vitro and in vivo, coinciding with defective glucose homeostasis. CDKAL1 mutant insulin+ cells were also hypersensitive to glucolipotoxicity. A high-content chemical screen identified a candidate drug that rescued CDKAL1 specific defects in vitro and in vivo by inhibiting the FOS/JUN pathway. Our approach of a proof-of-principle platform, which uses isogenic hESCs for functional evaluation of GWAS-

*Contact: Shuibing Chen shc2034@med.cornell.edu.

ΔThese authors contribute equal to the manuscript.

AUTHOR CONTRIBUTIONS

S.C., H.Z., J.G., T.E. designed the project, H. Z. and M. G. performed most experiments, T. Z., L. T., C. N. C., X. D., A. Y. and L. Y. performed other necessary experiments, T. Z. and J. Z. X. performed the bioinformatics analysis, H. Z., M. G., and S.C. analyzed data, H. Z., S.C. J.G., Q.Q. and T.E. wrote the manuscript.

identified loci and identification of a drug candidate that rescues gene-specific defects, paves the way for precision therapy of metabolic diseases.

eTOC Blurb

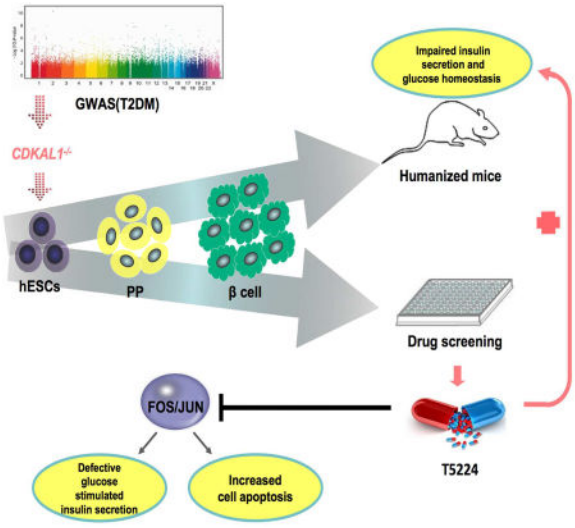

Zeng et al. report functional evaluation of GWAS identified candidate diabetes genes in an isogenic hESC-based platform. The authors find that biallelic mutations in *CDKAL1, KCNQ1*, and *KCNJ11* caused impaired insulin secretion both *in vitro* and *in vivo*, and identified the compound T5224 which rescued mutant *CDKAL1* associated pancreatic beta cell defects by inhibiting the *FOS/JUN* pathway.

INTRODUCTION

Multiple genome wide association studies (GWAS) have correlated Type 2 Diabetes Mellitus (T2DM) with genetic variants, yielding a large number of loci and associated gene products that are linked to the disease phenotype – often with little or no insight into the mechanism underlying that link (Hivert et al., 2014). The current challenge is to establish robust systems to systematically evaluate the role of these loci using disease relevant cells. Previous studies have used patient samples, cell lines, or animal models to seek mechanistic insight, but with significant limitations. Large variation is observed in primary patient samples, perhaps due to genetic heterogeneity, while animal models present major physiological and metabolic differences that hamper understanding of the precise function of human genes in T2DM. Therefore, a robust system to systematically evaluate the role of T2DM-associated genes using disease-relevant human cells will provide an important tool for diabetes research and spur the development of precision (allele-specific) therapies, exemplified by the use of sulfonylurea drugs to treat patients carrying certain *KCNJ11* mutations (Gloyn et al., 2004).

Human embryonic stem cells (hESCs) and human induced pluripotent stem cells (hiPSCs) provide platforms to recapitulate cellular pathology of human diseases. While two iPSC models have been used to mimic pancreatic beta cell defects in neonatal and inherited forms of diabetes: Maturity Onset Diabetes of Young 2 (Hua et al., 2013) and Wolfram Syndrome

patients (Shang et al., 2014), there is no robust model reported for T2DM-associated loci in the literature. Here, we focused on *CDKAL1, KCNQ1*, and *KCNJ11 loci* that were identified and confirmed through the first wave of T2DM GWAS. Risk alleles of the genetic variants at these loci are associated with aspects of beta cell function (HOMA-B) rather than insulin resistance (HOMA-IR) (Saxena et al., 2007; Scott et al., 2007; Steinthorsdottir et al., 2007; Unoki et al., 2008; Yasuda et al., 2008). Some studies suggested potential roles of these genes in pancreatic beta cell function or survival. For example, knockdown of *Cdkal1* enhanced endoplasmic reticulum (ER) stress in insulinoma cells (Brambillasca et al., 2012), while *Cdkal1*$^{-/-}$ mice show reduced first phase insulin exocytosis (Ohara-Imaizumi et al., 2010) and are hypersensitive to high fat diet-induced ER stress (Wei et al., 2011) and defects in glucose-stimulated insulin secretion (Okamura et al., 2012).

For other T2DM-linked genes, population and rodent studies reported mixed or even conflicting results. The risk allele of lead SNP at *KCNQ1* is associated with impaired insulin secretion (Unoki et al., 2008; Yasuda et al., 2008) and reduced insulin exocytosis in patients (Rosengren et al., 2012) and *Kcnq1*$^{-/-}$ mice have impaired glucose stimulated insulin secretion (GSIS)(Boini et al., 2009). However, forced expression of *Kcnq1* in an insulinoma cell line resulted in impairment of insulin secretion (Yamagata et al., 2011) and islets isolated from *Kcnq1*$^{-/-}$ mice revealed no difference in insulin secretion compared to wildtype islets (Asahara et al., 2015). Several activating mutations in *KCNJ11* result in permanent neonatal DM (Massa et al., 2005; Proks et al., 2004; Shimomura et al., 2006) and a polymorphism E23K is consistently linked with T2DM (Gloyn et al., 2003; Nielsen et al., 2003). A number of heterozygous mutations result in congenital hyperinsulinism (Bitner-Glindzicz et al., 2000). Heterozygous loss of murine *Kcnj11* causes a hyperinsulinaemic phenotype, whereas complete loss underlies eventual secretory failure (Remedi et al., 2006). These mixed results suggest that GWAS-identified genes may play a context dependent role in human pancreatic beta cells. Furthermore, using mouse models, it can be challenging to differentiate whether the GWAS-associated alteration causes cell autonomous defects or acts indirectly through extra-pancreatic tissues.

We built on recent work deriving glucose-responsive pancreatic beta-like cells from hESCs/iPSCs (Pagliuca et al., 2014; Rezania et al., 2014) and used isogenic hESC-derived glucose-responding cells to systematically examine the role of several GWAS-identified genes in pancreatic beta cell function and survival. While the mutations do not affect the generation of insulin^{+} cells, they impaired insulin secretion both *in vitro* and *in vivo*, coinciding with defective glucose homeostasis. *CDKAL1*$^{-/-}$ insulin^{+} cells also displayed hypersensitivity to glucolipotoxicity. A high-content chemical screen identified a candidate drug that rescued *CDKAL1*$^{-/-}$-specific defects by inhibiting the *FOS/JUN* pathway. These studies represent a proof-of-principle for the use of isogenic hESC-derived cells to define the precise role of genes associated with disease though GWAS in human pancreatic beta cells, as well as the lead-compound identification for pharmacological intervention of T2DM.

RESULTS

Generation of Biallelic Mutant hESC Lines by CRISPR-Cas9 Gene Targeting

We targeted indel mutations to *CDKAL1, KCNQ1*, or *KCNJ11* in INS$^{GFP/W}$ HES3 cells, since this reporter line allows for the purification of insulin producing (insulin^{+}) cells (Micallef et al., 2012). First, qRT-PCR was used to monitor the expression of the targeted genes in insulin-GFP^{+} cells derived from INS$^{GFP/W}$ HES3 cells. The transcript levels of C*DKAL1, KCNQ1*, and *KCNJ11* were detected at levels comparable to those observed in primary human adult beta cells (Figure 1A), suggesting that these genes are likely to function in the insulin^{+} cells.

To mutate each gene, INS$^{GFP/W}$ HES3 cells were electroporated with a vector expressing Cas9 and a specific sgRNA targeted to the first or second exon of each gene (Table S1). After sub-cloning, an efficiency of 11–15% (Table S2) was observed for the creation of biallelic mutant lines. Multiple independent clones for each mutation were expanded. All established clones have typical hESC colony morphology and express pluripotency markers, including OCT3/4, NANOG, TRA-1-60 and TRA-1-81 (Figure S1A). To account for possible variation between different clones, two clones (#1 and #2) were chosen of each mutant line for further analysis. Biallelic indel mutations for each of the targeted genes were verified by genomic DNA sequencing (Figure S1B). Each indel mutation creates an early frame-shift that is predicted to generate null alleles. Western blotting experiments further validated the knockout of the target genes in day 30 (D30) differentiated cells derived from each mutant hESC line (Figure 1B).

Biallelic Mutation of *CDKAL1, KCNQ1*, or *KCNJ11* Does Not Affect the Stepwise Differentiation towards Insulin^{+} Cells or the Expression of More Mature Beta Cell Markers

The isogenic lines were differentiated using a strategy modified slightly from a previously reported protocol (Rezania et al., 2014), which is summarized in Table S3. Immunocytochemistry analysis with antibodies against stage-specific markers was used to quantify differentiation efficiency. No significant difference was detected between wildtype and any of the isogenic mutant lines with respect to their capacity to differentiate toward definitive endoderm (SOX17^{+}/FOXA2^{+}, DE) (Figures S1C and S1D) or pancreatic progenitors (PDX1^{+}/NKX6.1^{+}/SOX9^{+}, PP) (Figures S1E–S1H). Flow cytometry analysis showed the percentage of insulin-GFP^{+} cells in D30 populations to be indistinguishable between wildtype and the isogenic mutant lines (Figure 1C; Figure S1I). Together, these data suggest that biallelic mutation of *CDKAL1, KCNQ1* or *KCNJ11* does not affect the stepwise differentiation of insulin^{+} cells.

The expression of pancreatic beta cell makers in D30 hESC-derived insulin^{+} cells was analyzed by immunocytochemistry, and all cells, regardless of genotype, were found to express markers indicative of mature pancreatic beta cells, including PDX1, NKX6.1 and NKX2.2 (Figure 1D). Intracellular FACS analysis showed that most hESC-derived insulin^{+} cells express the mature beta cell marker NKX6.1, but not the alpha cell marker glucagon (Figure 1E; Figure S1J). Wildtype and isogenic mutant cell lines did not differ with respect to the NKX6.1^{+}/insulin^{+} cell or insulin^{+}/glucagon^{-} cell fractions (Figure 1E; Figure S1J).

Next, insulin-GFP$^+$ cells were purified by cell sorting and analyzed for transcript expression levels with qRT-PCR (Figure S1K). Undifferentiated hESCs served as a negative control and primary human islets as a positive control. Transcripts encoding mature pancreatic beta cells markers, including *NKX6.1, NKX2.2, PDX1, ISLET1, PAX6, NEUROD1, GCK, G6PC2, UCN3* and *MAFA* are highly expressed at levels comparable to human islets in hESC-derived insulin-GFP$^+$ cells. No significant difference was observed between wildtype and isogenic mutant insulin-GFP$^+$ cells (Figure S1K). The total c-peptide level of wildtype and mutant hESC-derived insulin-GFP$^+$ cells, as measured by ELISA, was comparable to levels in primary human islets (Figure 1F, Table S4). Thus, mutation of *CDKAL1, KCNQ1*, or *KCNJ11* does not significantly affect the generation of mature beta-like cells or insulin production.

Mutation of *CDKAL1, KCNQ1* or *KCNJ11* Differentially Impairs Insulin Secretion in Response to Multiple Secretagogues

The major function of pancreatic beta cells is to secret insulin/c-peptide upon induction by secretagogues. D30 differentiated wildtype or mutant cells were stimulated with 30 mM KCl, and secreted human c-peptide was measured by ELISA. Wildtype cells respond with a 4.5±1.6 fold induction of c-peptide secretion (Figures 2A and 2B; Figure S2A). *CDKAL1*$^{-/-}$ cells showed a small but insignificant decreased response, while *KCNQ1*$^{-/-}$ and *KCNJ11*$^{-/-}$ cells were severely and significantly impaired in their response to KCl stimulation (Figures 2A and 2B). The cells were further queried for their response to 10 mM arginine. Again, both wildtype and *CDKAL1*$^{-/-}$ D30 cells responded well, while *KCNQ1*$^{-/-}$ and *KCNJ11*$^{-/-}$ cells failed to respond (Figures 2C and 2D; Figure S2B). D30 cells were also stimulated with 20 μM forskolin or 50 μM IBMX to measure cAMP induced insulin secretion. Wildtype cells responded well to both, yielding 7.2±1.9 and 6.2±1.8 fold induction of c-peptide secretion, respectively (Figures 2E and 2F; Figure S2C). Cells carrying the three mutant alleles were able to respond to both forskolin and IBMX stimulation (Figure 2E), but compared to wildtype cells the fold induction was significantly decreased (Figure 2F). Finally, wildtype cells stimulated with 2 mM (low) or 20 mM (high) D-glucose responded to high glucose with a 2.3±0.8 fold induction of c-peptide secretion, while all three mutant genotypes failed to respond (Figures 2G and 2H, Figure S2D). Thus, loss of *KCNQ1* or *KCNJ11* affects insulin secretion. Since *CDKAL1*$^{-/-}$ cells respond to KCl and arginine (Figures 2A and 2C), but not cAMP or glucose stimulation (Figures 2E and 2G), CDKAL1 may be involved in cAMP and glucose sensing rather than exocytosis of insulin granules.

Patch-Clamp experiments were used to determine K_{ATP} channel activity in *KCNJ11*$^{-/-}$ cells. To perform K_{ATP} current recordings, wildtype insulin-GFP$^+$ cells were held at 0 mV to inactivate any voltage gated ion channels, and K_{ATP} currents were elicited by depolarization from HP=0 mV to +80 mV. K_{ATP} channels were activated by the K_{ATP} channel-specific activator diazoxide (Pasyk et al., 2004) (Figure S2E), and inhibited by K_{ATP} channel-specific blocker glybenclamide. The effect of diazoxide was reversible. After washout of diazoxide, glybenclamide further reduced current amplitude from 400 pA to ~ 200 pA (Figure S2F), suggesting that in the absence of diazoxide, there were basal K_{ATP} channel activities, which was likely induced by the pipette solution. Whereas K_{ATP} currents were recorded in wildtype insulin-GFP$^+$ cells, diazoxide and glybenclamide did not produce any effects in the

recordings from insulin-GFP$^+$ *KCNJ11*$^{-/-}$ mutant cells (Figure S2G), suggesting the absence of K_{ATP} channel activity.

CDKAL1$^{-/-}$ Insulin-GFP$^+$ Cells are Hypersensitive to Glucolipotoxicity

Hyperglycemia and hyperlipidemia are two major risk factors associated with pancreatic beta cell death in diabetic patients. Wildtype and isogenic *CDKAL1*$^{-/-}$, *KCNQ1*$^{-/-}$, and *KCNJ11*$^{-/-}$ D30 insulin-GFP$^+$ cells were cultured in the presence of 35 mM D-Glucose for 96 hours, or 1 mM palmitate for 48 hours. Cells were stained with propidium iodide (PI) to determine the cell death rate (Figure 3A). No significant difference was detected between wildtype and mutant insulin$^+$ cells under control conditions. However, the percentage of PI$^+$/insulin$^+$ cells in *CDKAL1*$^{-/-}$ insulin$^+$ cells was significantly higher compared to wildtype insulin$^+$ cells exposed to 35 mM D-Glucose or 1 mM palmitate, indicating that *CDKAL1*$^{-/-}$ insulin$^+$ cells are hypersensitive to glucotoxicity and lipotoxicity (Figure 3B). In contrast, neither *KCNQ1*$^{-/-}$ nor *KCNJ11*$^{-/-}$ insulin$^+$ cells showed increased sensitivity to glucotoxicity or lipotoxicity (Figure S3A). Treated cells were stained with the apoptosis marker Annexin V, as well as the cell death marker 7AAD and evaluated by flow cytometry to measure apoptosis in insulin-GFP$^+$ cells (Figure 3C and S3B). Consistent with the PI staining results, the percentage of Annexin V$^+$/7AAD$^-$ cells in *CDKAL1*$^{-/-}$ insulin-GFP$^+$ cells was significantly higher than wildtype (Figure 3D), *KCNQ1*$^{-/-}$ or *KCNJ11*$^{-/-}$ insulin-GFP$^+$ cells when cultured in the presence of 35 mM D-Glucose or 1 mM palmitate (Figure S3C and S3D). We also measured the proliferation rate of wildtype and *CDKAL1*$^{-/-}$ insulin-GFP$^+$ cells (Figure S3E), which showed no significant difference (Figure S3F). RNA-seq was used to compare the gene expression profiles in wildtype and *CDKAL1*$^{-/-}$ cells cultured in the presence or absence of palmitate. ER stress-related genes were found significantly upregulated in *CDKAL1*$^{-/-}$ cells cultured under palmitate conditions (Figures 3E and 3F). This suggests, consistent with the literature (Brambillasca et al., 2012; Wei et al., 2011), that loss of CDKAL1 induces elevated ER stress under exposure to high levels of fatty acids.

CDKAL1$^{-/-}$, *KCNQ1*$^{-/-}$, and *KCNJ11*$^{-/-}$ hESC-Derived Beta-Like Cells Show Defective GSIS and Impaired Capacity to Maintain Glucose Homeostasis *in vivo*

To determine the survival and functional capacities of *CDKAL1*$^{-/-}$, *KCNQ1*$^{-/-}$, and *KCNJ11*$^{-/-}$ hESC-derived beta-like cells *in vivo*, wildtype and isogenic mutant glucose-responding cells were transplanted under the kidney capsule of immuno-deficient SCID-Beige mice. Two days after transplantation, the mice were treated with 200 mg/kg streptozotocin (STZ) to chemically ablate endogenous murine pancreatic beta cells (Figure S4A). After STZ treatment, the levels of mouse insulin are below the detection limit of the ELISA kit (Figure S4B). Two weeks post-transplantation, SCID-beige mice carrying human cells were fasted overnight and monitored for GSIS, measuring by ELISA human insulin in serum at fasting and 30 min after stimulation with 3 g/kg glucose (Figure 4A and S4C). SCID-beige mice transplanted with wildtype or mutant cells displayed indistinguishable concentrations of human insulin (Figure 4A). By six weeks post transplantation, SCID-beige mice carrying wildtype cells showed significantly increased insulin secretion after glucose stimulation (Figure 4B; Figure S4D), while SCID-beige mice carrying *CDKAL1*$^{-/-}$, *KCNQ1*$^{-/-}$, or *KCNJ11*$^{-/-}$ cells continued to fail to respond to glucose stimulation (Figure 4B). Since SCID-beige mice transplanted with wildtype or mutant cells displayed

indistinguishable concentrations of human insulin at two weeks after transplantation (Figure 4A), the failed GSIS of mice carrying mutant cells at 6 weeks after transplantation is due to the impaired function of the transplanted cells, rather than unsuccessful transplantation. These results validate *in vivo* the impaired glucose response measured in mutant cells *in vitro* (Figure 2G).

To monitor the capacity of the transplanted cells to maintain glucose homeostasis in STZ-treated mice beyond an acute glucose response, an intraperitoneal glucose tolerance test (IPGTT) with 2 g/kg glucose was used. In contrast to SCID-beige mice carrying wildtype cells, those transplanted with *CDKAL1*$^{-/-}$, *KCNQ1*$^{-/-}$, or *KCNJ11*$^{-/-}$ cells show glucose intolerance (Figure 4C; Figure S4E). The area under the curve (AUC) for the glucose tolerance test in SCID-beige mice carrying mutant cells was significantly higher compared to that of SCID-beige mice carrying wildtype cells (Figure 4D; Figure S4F). Immunohistochemistry was used to document the persistence of human beta-like cells in transplanted human grafts. Mature pancreatic beta cells markers, including PDX1, NKX6.1, NKX2.2 and insulin were detected in the grafts regardless of genotype (Figure S4G). Taken together, beta-like cells derived from *CDKAL1*$^{-/-}$, *KCNQ1*$^{-/-}$, or *KCNJ11*$^{-/-}$ hESCs present with impaired glucose induced insulin secretion as well as glucose tolerance in SCID-beige mice carrying glucose-responding cells.

A High Content Chemical Screen Identifies A Candidate Drug That Rescues *CDKAL1*$^{-/-}$ Specific Glucolipotoxicity and Impaired GSIS

A high content chemical screen was performed to identify drug candidates capable of rescuing *CDKAL1*$^{-/-}$ specific glucolipotoxicity. D30 differentiated *CDKAL1*$^{-/-}$ cells were replated in 384-well plates and treated for 48 hours with chemicals from a collection of FDA-approved drugs and drug candidates in clinical trials at 10 μM in the presence of 1 mM palmitate. We screened 2000 compounds for the capacity to decrease cell death by at least 80% in *CDKAL1*$^{-/-}$ derived beta-like cells exposed to glucolipotoxicity, while also increasing the number of insulin^{+} cells at least two-fold (Figure S5A). Of six initial lead hits, one compound, T5224 (Figure 5A) was validated to protect *CDKAL1*$^{-/-}$ insulin^{+} cells from glucolipotoxicity in follow up experiments. Using the same platform as for the primary screening (1 mM palmitate), addition of T5224 caused increased numbers of insulin^{+} cells (Figure 5B) and a decreased percentage of PI^{+}/INS^{+} cells in *CDKAL1*$^{-/-}$ insulin^{+} cells (Figures 5C) in a dose-dependent manner with an EC_{50} of 16.2 μM. In addition, T5224 rescued the increased the cell death rate in *CDKAL1*$^{-/-}$ insulin^{+} cells when cultured with high glucose or high palmitate (Figure 5D and 5E). As measured using the Annexin V assay for apoptosis, T5224 also rescued the increased apoptotic rate in *CDKAL1*$^{-/-}$ insulin^{+} cells under conditions of high fatty acid concentration, without affecting the rate in wildtype insulin^{+} cells (Figures 5F and 5G; Figure S5B), thus blunting hypersensitivity to glucolipotoxicity.

The *CDKAL1*$^{-/-}$ cells were treated with 30 μM T5224 for 48 hours and examined for impaired response to forskolin or glucose stimulated insulin secretion (FSIS and GSIS). Remarkably, the mutant cells treated with T5224 showed increased insulin secretion in response to forskolin treatment (Figure 5H and Figure S5C), significantly elevated compared

to cells treated with DMSO and at a level of insulin secretion comparable to wildtype cells (Figure 5H). Similarly, T5224 treatment also rescued the impaired GSIS of *CDKAL1*$^{-/-}$ cells (Figure 5I and Figure S5D). Notably, T5224 treatment did not significantly affect FSIS or GSIS in wildtype cells.

T5224 Rescues *CDKAL1*$^{-/-}$ Induced Beta Cell Defects Through Inhibition of The *FOS/JUN* Pathway

T5224 was reported to be an inhibitor of FOS/JUN activator protein-1 (AP-1) (Aikawa et al., 2008). To explore this potential mechanism of action, RNA-seq was used to compare the global gene expression profiles in *CDKAL1*$^{-/-}$ and wildtype insulin-GFP^{+} cells. Pathway enrichment analysis highlighted the *FOS/JUN* and *Focal Adhesion* pathways as highly changed in *CDKAL1*$^{-/-}$ insulin-GFP^{+} cells (Figure 6A). Genes associated with the *Focal Adhesion* GO term were consistently downregulated (Figure 6B and Figure S6A) while the *FOS/JUN* pathway (Figure 6C) was consistently upregulated in *CDKAL1*$^{-/-}$ insulin-GFP^{+} cells. Among the top 20 genes showing relatively increased expression in *CDKAL1*$^{-/-}$ insulin-GFP^{+} cells are *FOSB* (6.3 fold), *FOS* (3.5 fold), and *JUNB* (2.4 fold) (Figure 6D), which was confirmed by qRT-PCR (Figure 6E). Finally, western blotting experiments validated the relatively increased expression of FOS protein in mutant cells (Figure 6F).

To determine whether the mutation of *CDKAL1* induces pancreatic beta cell defects through activation of the *FOS/JUN* pathway, two sgRNAs and two scrambled sgRNAs were designed to knockout human *FOS* (Table S6). Wildtype and *CDKAL1*$^{-/-}$ hESC-derived day 10 PPs were infected with lentivirus expressing either sgFOS, or a scrambled sgRNA and following 4–6 days selection with puromycin, the cells were differentiated to beta-like cells for an additional 16–20 days. In cells expressing sgFOS, the expression of FOS was decreased by more than 99% based on western blotting experiments, validating the targeting efficiency (Figure S6B). The cells were cultured in the absence or presence of 35 mM D-glucose or 1 mM palmitate and analyzed with respect to the rates of cell death and apoptosis by PI staining and Annexin V, respectively. Mutation of *FOS* using sgRNA rescues the increased cell death rate of *CDKAL1*$^{-/-}$ insulin-GFP^{+} cells (Figure 6G), and cell apoptotic rate of *CDKAL1*$^{-/-}$ insulin-GFP^{+} cells (Figures 6H and 6I; Figure S6C). In contrast, mutation of *FOS* does not affect cell death (Figure 6G) or apoptosis in wildtype insulin-GFP^{+} cells (Figures 6H and 6I). In addition to sgRNA, two shRNA against *FOS* were cloned into a lentivirial vector and used to knockdown *FOS*. The knockdown efficiency in day 10 PPs is more than 50% based on western blotting experiments (Figure S6D). Consistent with the knockout using sgFOS, knockdown of FOS using shRNAs rescued the increased cell apoptotic rate of *CDKAL1*$^{-/-}$ insulin-GFP^{+} cells when cultured in high fatty acid condition (Figures S6E and S6F).

Likewise, wildtype and *CDKAL1*$^{-/-}$ hESC-derived PPs infected with lentivirus expressing sgFOS or a scrambled sgRNA were differentiated for 20 days and measured for FSIS and GSIS. *CDKAL1*$^{-/-}$ cells infected with lentivirus containing scrambled sgRNA showed impaired FSIS and GSIS compared to wildtype cells. Transfection with lentivirus expressing sgFOS rescued those phenotypes (Figures 6J and 6K; Figures S6G and S6H). However, knockout of FOS did not affect FSIS (Figure 6J) or GSIS (Figure 6K) in wildtype cells.

Consistently, knockdown of *FOS* using shRNAs recued the impaired FSIS (Figures S6I and S6K) and GSIS (Figures S6J and S6L) in *CDKAL1*$^{-/-}$ cells without affecting wildtype cells. Together, this suggests that loss of *CDKAL1* causes hypersensitivity to glucolipotoxicity and impairs FSIS and GSIS through the *FOS/JUN* pathway.

T5224 and Loss of *FOS* Rescues the Function of *CDKAL1*$^{-/-}$ Cells *in vivo*

To examine the effect of T5224 on *CDKAL1*$^{-/-}$ cells *in vivo*, mice transplanted with wildtype and *CDKAL1*$^{-/-}$ cells were examined for GSIS at 10 weeks after transplantation. Consistent with the 6 week results reported above, mice transplanted with wildtype cells respond well to glucose stimulation. In contrast, mice transplanted with *CDKAL1*$^{-/-}$ cells showed impaired GSIS (Figure 7A and S7A). After glucose stimulation, the insulin level of mice transplanted with *CDKAL1*$^{-/-}$ cells was significantly lower than for mice transplanted with wildtype cells.

Subsequently, mice were treated with 300 mg/kg T5224 orally and measured for GSIS 48 hours after treatment. Mice treated with T5224 restored the capacity to respond to glucose stimulation (Figure 7B and S7B). T5224 treatment significantly increased the level of insulin secretion after glucose stimulation. In addition, the mice carrying *CDKAL1*$^{-/-}$ cells showed glucose intolerance. T5224 treatment restored the capacity of the SCID-beige mice carrying human cells to maintain glucose homeostasis (Figure 7C and S7C). The AUC for mice after T5224 treatment was significantly lower than for mice treated with control vehicle (Figure 7D and S7D). T5224 treatment was also examined using mice carrying wildtype cells. Consistent with the *in vitro* results (Figure 5), T5224 treatment affects neither GSIS (Figure S7E and S7F) nor glucose tolerance of mice carrying wildtype cells (Figure S7G–S7J). To determine the long-term effect of T5224, mice carrying *CDKAL1*$^{-/-}$ cells were treated with 300 mg/kg T5224 orally twice a week and measured for GSIS and glucose tolerance 4 weeks after treatment. The long-term treatment of T5224 restored both GSIS (Figure 7E and S7K) and glucose tolerance (Figure 7F, 7G and S7L, S7M) for mice carrying *CDKAL1*$^{-/-}$ cells. Finally, D30 *CDKAL1*$^{-/-}$ cells carrying scrambled sgRNA, and D30 *CDKAL1*$^{-/-}$ cells carrying sgFOS were transplanted into mice that were than measured for function *in vivo* 6 weeks after transplantation. Consistent with *in vitro* results (Figure 6), mice with *CDKAL1*$^{-/-}$ cells carrying sgFOS showed improved GSIS (Figure 7H and S7N) and a stronger ability to maintain glucose homeostasis (Figure 7I, 7J and S7O and S7P) than mice transplated with *CDKAL1*$^{-/-}$ cells carrying scrambled sgRNA. Together, these data suggest that T5224 or loss of FOS rescues the function of *CDKAL1*$^{-/-}$ cells *in vivo*.

DISCUSSION

With more than 80 loci associated with T2DM identified by GWAS, a robust platform to evaluate the role of these loci using disease relevant cells is urgently needed. Here we report proof-of-principle for using isogenic hESC-derived glucose-responding cells to evaluate the role of these loci in the function and survival of human pancreatic beta cells under conditions mimicking both health and disease. The derived glucose-responding cells share the same genetic background, providing a unique resource to determine the precise role of

genes or loci in human pancreatic beta cells independent of complications from genetic heterogeneity implied by other approaches such as patient-derived iPSCs.

We found that mutation of *KCNJ11* resulted in impaired insulin secretion upon KCl, arginine, forskolin, IBMX, and glucose stimulation, suggesting that *KCNJ1*1 plays an essential role in insulin secretion, which is consistent with results in homozygous *Kcnj11*$^{-/-}$ KO mice, as well as in homozygous *Kcnj11*$^{-/-}$ null mice (Remedi et al., 2006) (Boini et al., 2009). In the context of reports that forced expression of *KCNQ1* in a mouse beta cell line results in impairment of insulin secretion (Yamagata et al., 2011) and islets isolated from *Kcnq1*$^{-/-}$ mice reveal no difference in the extent of basal or stimulated insulin secretion compared to islet from wildtype mice (Asahara et al., 2015), we were surprised to find impaired insulin secretion in *KCNQ1*$^{-/-}$ insulin-secreting cells. This apparent discrepancy may suggest dose and/or species-specific roles in pancreatic beta cell function, highlighting the importance of using human relevant cell types.

An ultimate goal of exploring loci or genetic variants associated with disease through GWAS is to identify locus/variant-specific treatments. Risk alleles of SNPs at the *CDKAL1* locus associated with diabetes are thought to be loss-of-function alleles, which we modeled generating null mutations. We found that *CDKAL1*$^{-/-}$ insulin^{+} cells showed impaired FSIS and GSIS, which is consistent with *Cdkal1*$^{-/-}$ mice showing reduced first phase insulin exocytosis (Ohara-Imaizumi et al., 2010). *CDKAL1*$^{-/-}$ insulin^{+} cells also show increased ER stress, cell apoptosis and death when cultured in high glucose and high fatty acid conditions. Although there are papers describing the potential contribution of lipotoxicity in T2DM, direct evidence that lipotoxicity affect pancreatic beta cell death *in vivo* under normal physiological and pathological conditions needs to be further explored. Here, we found that *CDKAL1*$^{-/-}$ insulin^{+} cells are hypersensitive to both high glucose and high fatty acid induced pancreatic beta-like cell death. Moreover, *CDKAL1*$^{-/-}$ insulin^{+} cells display defective GSIS and impaired ability to maintain glucose homeostasis following transplantation into STZ-treated mice. This is consistent with the *in vitro* functional defects of *CDKAL1*$^{-/-}$ insulin^{+} cells. Since the mice are hyperglycemic after STZ treatment, the observed glucotoxicity may further worsen the defects of *CDKAL1*$^{-/-}$ insulin^{+} cells. From a high content chemical screen, T5224 was found to rescue the *CDKAL1* mutation-mediated pancreatic beta cell defects. T5224 has been investigated in clinical trials for patients with rheumatoid arthritis (Adis, 2014) and may have the potential to be repurposed for *CDKAL1*-specific treatment of T2DM. T5224 is able to strikingly rescue *CDKAL1* mutation-mediated pancreatic beta cell dysfunction *in vivo*, which is a proof-of-concept for a T2DM drug candidate rescuing a gene-specific defect *in vivo*.

By combining high content chemical screening and RNA-seq, we found the *FOS/JUN* pathway to be significantly upregulated in *CDKAL1*$^{-/-}$ insulin^{+} cells, and that reducing *FOS/JUN* pathway activity either chemically or genetically rescued *CDKAL1* mutation-induced defects. Previous studies have shown that *FOS/JUN* activation is involved in cytokine and mechanical stress-induced beta cell death (Abdelli et al., 2007; Hughes et al., 1990) and amylin-induced apoptosis (Zhang et al., 2002). Here, we found that *CDKAL1*$^{-/-}$ mediated activation of the *FOS/JUN* pathway through fatty acids may be a further effector of

FOS/JUN regulated beta cell survival, providing mechanistic insight into how *CDKAL1* locus may contribute to diabetes progression.

In summary, we established an isogenic hESC platform to systematically evaluate the role of disease-associated loci in the survival and function of human pancreatic beta-like cells *in vitro* and *in vivo*. The platform can be used to study other disease-associated loci/variants with respect to beta-like cell function. It is worth noting that the glucose-responding cells derived using the current reported protocols are not equivalent to primary human beta cells. Ca^{2+} flux assays suggested that approximately 30–40% of the insulin-GFP^{+} cells show increased cytosolic Ca^{2+} concentrations in response to glucose stimulation (Figure. S7Q), whereas robust glucose-induced signaling was observed in more than 70% of human beta cells, based on the previous report (Rezania et al., 2014). The restricted functionality of pancreatic beta-like cells derived using current protocols might limit their application for evaluating subtle contributions of genes to glucose metabolism and Ca^{2+} signaling. Thus, additional work is needed to further improve the protocol to derive mature pancreatic beta-like cells. In addition, the platform established here can also be applied to study the role of disease-associated loci/variants in other diabetes-related cell types, such as hepatocytes, adipocytes, muscles and/or intestinal neuroendocrine cells. Finally, the system may be used as a high throughput/content chemical screening platform to identify candidate drugs correcting allele-specific defects, for precision therapy of metabolic diseases.

EXPERIMENTAL PROCEDURES

Cell Culture and Chemicals

All experiments were performed using INS^{GFPW} HES3 cells. hESCs were grown on Matrigel-coated 6-well plates in mTeSR1 medium (STEM CELL Technologies). Cells were maintained at 37°C with 5% CO2. T5224 was purchased from MedChem Express (HY-12270). Human islets were provided by IIDP (Integated Islet Distribution Program).

Creation of Isogenic Mutant hESC Lines

To mutate the target genes, two sgRNAs targeting the first two exons of the target gene were designed, cloned into a vector carrying a CRISPR-Cas9 gene, and validated using the surveyor assay in 293T cells. After validation, $INS^{GFP/W}$ HES3 cells were dissociated using Accutase (STEM CELL Technologies) and transfected (8×10^5 cells per sample) in suspension using Human Stem Cell Nucleofector™ solution (Lonza) using electroporation and following the manufacturer's instructions. Cells were co-transfected with the vector expressing Cas9/sgRNA at 10 nM final concentration and a vector expressing puromycin. After replating, the transfected cells were treated with 500 ng/ml puromycin. After two days of puromycin selection, hESCs were dissociated into single cells by Accutase and re-plated at low density. 10 μM Y-27632 was added. After approximately 10 days, individual colonies were picked, mechanically disaggregated and re-plated into two individual wells of 96-well plates. A portion of the cells was analyzed by genomic DNA sequencing. For biallelic frameshift mutants, we chose both homozygous mutants and compound heterozygous mutants. Wild-type clonal lines from the corresponding targeting experiments were included

as wild-type controls to account for potential nonspecific effects associated with the gene targeting process.

Stepwise Differentiation

Wildtype and isogenic mutant hESCs were differentiated using either of two slightly modified protocols from what was previously reported (Rezania et al., 2014). The details of protocol 1 and 2 are listed as supplemental Figure 1C and described in detail in supplemental methods.

In vivo Transplantation, GSIS and IPGTT

Wildtype and isogenic mutant hESCs at day 30 of differentiation were resuspended in 40 μl DMEM+B27 and transplanted under the kidney capsule of 6–8 week old male SCID-beige mice. Two days after transplantation, the mice were treated with 200 mg/kg STZ. To perform GSIS, mice were starved for about 20 hours. Mouse blood was collected under fasting conditions and at 15 min after intraperitoneal injection with 3 g/kg glucose solution. The mouse sera were analyzed using the ultrasensitive human insulin ELISA kit (ALPCO, 80-INSHUU-E01.1). To perform IPGTT analysis, the mice were fasted overnight and treated with 2 g/kg glucose. Blood glucose level (mg/dl) in each animal was measured before and every 15 minutes in the first hour and every 30 minutes in the second hour after glucose injection. The mice transplanted with wildtype or *CDKAL1*$^{-/-}$ cells were orally treated with 300 mg/kg T5224 dissolved in polyvinylpyrrolidone K 60 solution (Sigma). After 48 hours treatment, the mice were examined for GSIS and IPGTT. The mice treated with polyvinylpyrrolidone K 60 solution (vehicle) were used as the controls. For long-term treatment, the mice were orally treated with 300 mg/kg T5224 twice a week for four weeks. GSIS and IPGTT were measured 48 hours after the last treatment.

High Content Chemical Screening

To perform the high content chemical screening, *CDKAL1*$^{-/-}$ D30 cells were plated on 804G-coated 384 well plates at 5000 cells/40 μl medium/well. After overnight incubation, cells were treated at 10 μM with compounds from a chemical collection containing the Prestwick FDA approved drug library and drugs in clinical trials. DMSO treatment was used as a negative control. After 48 hours incubation, cells were first stained with 100 μg/ml PI and then fixed and stained using an insulin antibody (DAKO). Plates were analyzed using a Molecular Devices ImageXpress High-Content Analysis System. Two dimensional analysis was used. Compounds decreasing the cell death rate in excess of 80% and increasing the number of insulin^{+} cells by 2-fold were picked as primary hits.

Statistical Analysis

n=3 independent biological replicates if not otherwise specifically indicated. n.s. indicates non-significant difference. *p* values were calculated by unpaired two-tailed Student's t-test if not otherwise specifically indicated. n=8 mice for *in vivo* experiments if not otherwise specifically indicated. *p* values were calculated by one-way repeated measures ANOVA or two-way repeated measures ANOVA with a Bonferroni test for multiple comparisons between wildtype and knockout cells. *$p<0.05$, **$p<0.01$, ***$p<0.001$, and ****$p<0.0001$.

Supplementary Material

Refer to Web version on PubMed Central for supplementary material.

Acknowledgments

S.C. is funded by The New York Stem Cell Foundation (R-103), American Diabetes Association (1-12-JF-06), Tri-institutional Starr Stem Cell Grant (2014-030). S.C. is New York Stem Cell Foundation-Robertson Investigator. T.Z. is funded by a NYSTEM postdoctoral fellowship. A.Y. and L. Y. are supported by NIH HL078960 (to L.Y.) and AHA grant 16GRNT26430113 (to L.Y.). J.G. was supported by "Biomedical Research Program" funds at Weill Cornell Medical College in Qatar, a program funded by Qatar Foundation. Q. Q. is supported by a Scientist Development Award (K01HL129892) from the NHLBI. This study was also supported by a Shared Facility contract to T.E. and S.C. from the New York State Department of Health (NYSTEM C029156). NKX6.1 and NKX2.2 antibodies were provided by U of lowa Hybridoma bank. Human islets were provided by The Integrated Islet Distribution Program. The plentiCRISPR v2 vector and Puro 2.0 were purchased from Addgene (plasmid#52961 and #24970). We are also very grateful for technical support and advice provided by Harold S. Ralph in the Cell Screening Core Facility and Jason McCormick in the Flow Cytometry Facility at Weill Cornell Medical College, NY. The authors have filled a patent "AP-1 inhibitors for precison therapy of diabetic pateints"

References

Abdelli S, Abderrahmani A, Hering BJ, Beckmann JS, Bonny C. The c-Jun N-terminal kinase JNK participates in cytokine- and isolation stress-induced rat pancreatic islet apoptosis. Diabetologia. 2007; 50:1660–1669. [PubMed: 17558486]

Adis. Drugs in Clinical Development for Rheumatoid Arthritis Summary and Table. Pharmaceutical Medicine. 2014; 28:195–213.

Aikawa Y, Morimoto K, Yamamoto T, Chaki H, Hashiramoto A, Narita H, Hirono S, Shiozawa S. Treatment of arthritis with a selective inhibitor of c-Fos/activator protein-1. Nature biotechnology. 2008; 26:817–823.

Asahara S, Etoh H, Inoue H, Teruyama K, Shibutani Y, Ihara Y, Kawada Y, Bartolome A, Hashimoto N, Matsuda T, et al. Paternal allelic mutation at the Kcnq1 locus reduces pancreatic beta-cell mass by epigenetic modification of Cdkn1c. Proceedings of the National Academy of Sciences of the United States of America. 2015; 112:8332–8337. [PubMed: 26100882]

Bitner-Glindzicz M, Lindley KJ, Rutland P, Blaydon D, Smith VV, Milla PJ, Hussain K, Furth-Lavi J, Cosgrove KE, Shepherd RM, et al. A recessive contiguous gene deletion causing infantile hyperinsulinism, enteropathy and deafness identifies the Usher type 1C gene. Nature genetics. 2000; 26:56–60. [PubMed: 10973248]

Boini KM, Graf D, Hennige AM, Koka S, Kempe DS, Wang K, Ackermann TF, Foller M, Vallon V, Pfeifer K, et al. Enhanced insulin sensitivity of gene-targeted mice lacking functional KCNQ1. American journal of physiology Regulatory, integrative and comparative physiology. 2009; 296:R1695–1701.

Brambillasca S, Altkrueger A, Colombo SF, Friederich A, Eickelmann P, Mark M, Borgese N, Solimena M. CDK5 regulatory subunit-associated protein 1-like 1 (CDKAL1) is a tail-anchored protein in the endoplasmic reticulum (ER) of insulinoma cells. The Journal of biological chemistry. 2012; 287:41808–41819. [PubMed: 23048041]

Gloyn AL, Pearson ER, Antcliff JF, Proks P, Bruining GJ, Slingerland AS, Howard N, Srinivasan S, Silva JM, Molnes J, et al. Activating mutations in the gene encoding the ATP-sensitive potassium-channel subunit Kir6.2 and permanent neonatal diabetes. The New England journal of medicine. 2004; 350:1838–1849. [PubMed: 15115830]

Gloyn AL, Weedon MN, Owen KR, Turner MJ, Knight BA, Hitman G, Walker M, Levy JC, Sampson M, Halford S, et al. Large-scale association studies of variants in genes encoding the pancreatic beta-cell KATP channel subunits Kir6.2 (KCNJ11) and SUR1 (ABCC8) confirm that the KCNJ11 E23K variant is associated with type 2 diabetes. Diabetes. 2003; 52:568–572. [PubMed: 12540637]

Hivert MF, Vassy JL, Meigs JB. Susceptibility to type 2 diabetes mellitus--from genes to prevention. Nature reviews Endocrinology. 2014; 10:198–205.

Hua H, Shang L, Martinez H, Freeby M, Gallagher MP, Ludwig T, Deng L, Greenberg E, Leduc C, Chung WK, et al. iPSC-derived beta cells model diabetes due to glucokinase deficiency. The Journal of clinical investigation. 2013; 123:3146–3153. [PubMed: 23778137]

Hughes JH, Watson MA, Easom RA, Turk J, McDaniel ML. Interleukin-1 induces rapid and transient expression of the c-fos proto-oncogene in isolated pancreatic islets and in purified beta-cells. FEBS letters. 1990; 266:33–36. [PubMed: 2114318]

Massa O, Iafusco D, D'Amato E, Gloyn AL, Hattersley AT, Pasquino B, Tonini G, Dammacco F, Zanette G, Meschi F, et al. KCNJ11 activating mutations in Italian patients with permanent neonatal diabetes. Human mutation. 2005; 25:22–27. [PubMed: 15580558]

Micallef SJ, Li X, Schiesser JV, Hirst CE, Yu QC, Lim SM, Nostro MC, Elliott DA, Sarangi F, Harrison LC, et al. INS(GFP/w) human embryonic stem cells facilitate isolation of in vitro derived insulin-producing cells. Diabetologia. 2012; 55:694–706. [PubMed: 22120512]

Nielsen EM, Hansen L, Carstensen B, Echwald SM, Drivsholm T, Glumer C, Thorsteinsson B, Borch-Johnsen K, Hansen T, Pedersen O. The E23K variant of Kir6.2 associates with impaired post-OGTT serum insulin response and increased risk of type 2 diabetes. Diabetes. 2003; 52:573–577. [PubMed: 12540638]

Ohara-Imaizumi M, Yoshida M, Aoyagi K, Saito T, Okamura T, Takenaka H, Akimoto Y, Nakamichi Y, Takanashi-Yanobu R, Nishiwaki C, et al. Deletion of CDKAL1 affects mitochondrial ATP generation and first-phase insulin exocytosis. PloS one. 2010; 5:e15553. [PubMed: 21151568]

Okamura T, Yanobu-Takanashi R, Takeuchi F, Isono M, Akiyama K, Shimizu Y, Goto M, Liang YQ, Yamamoto K, Katsuya T, et al. Deletion of CDKAL1 affects high-fat diet-induced fat accumulation and glucose-stimulated insulin secretion in mice, indicating relevance to diabetes. PloS one. 2012; 7:e49055. [PubMed: 23173044]

Pagliuca FW, Millman JR, Gurtler M, Segel M, Van Dervort A, Ryu JH, Peterson QP, Greiner D, Melton DA. Generation of functional human pancreatic beta cells in vitro. Cell. 2014; 159:428–439. [PubMed: 25303535]

Pasyk EA, Kang Y, Huang X, Cui N, Sheu L, Gaisano HY. Syntaxin-1A binds the nucleotide-binding folds of sulphonylurea receptor 1 to regulate the KATP channel. The Journal of biological chemistry. 2004; 279:4234–4240. [PubMed: 14645230]

Proks P, Antcliff JF, Lippiat J, Gloyn AL, Hattersley AT, Ashcroft FM. Molecular basis of Kir6.2 mutations associated with neonatal diabetes or neonatal diabetes plus neurological features. Proceedings of the National Academy of Sciences of the United States of America. 2004; 101:17539–17544. [PubMed: 15583126]

Remedi MS, Rocheleau JV, Tong A, Patton BL, McDaniel ML, Piston DW, Koster JC, Nichols CG. Hyperinsulinism in mice with heterozygous loss of K(ATP) channels. Diabetologia. 2006; 49:2368–2378. [PubMed: 16924481]

Rezania A, Bruin JE, Arora P, Rubin A, Batushansky I, Asadi A, O'Dwyer S, Quiskamp N, Mojibian M, Albrecht T, et al. Reversal of diabetes with insulin-producing cells derived in vitro from human pluripotent stem cells. Nature biotechnology. 2014; 32:1121–1133.

Rosengren AH, Braun M, Mahdi T, Andersson SA, Travers ME, Shigeto M, Zhang E, Almgren P, Ladenvall C, Axelsson AS, et al. Reduced insulin exocytosis in human pancreatic beta-cells with gene variants linked to type 2 diabetes. Diabetes. 2012; 61:1726–1733. [PubMed: 22492527]

Saxena R, Voight BF, Lyssenko V, Burtt NP, de Bakker PI, Chen H, Roix JJ, Kathiresan S, Hirschhorn JN, Daly MJ, et al. Genome-wide association analysis identifies loci for type 2 diabetes and triglyceride levels. Science. 2007; 316:1331–1336. [PubMed: 17463246]

Scott LJ, Mohlke KL, Bonnycastle LL, Willer CJ, Li Y, Duren WL, Erdos MR, Stringham HM, Chines PS, Jackson AU, et al. A genome-wide association study of type 2 diabetes in Finns detects multiple susceptibility variants. Science. 2007; 316:1341–1345. [PubMed: 17463248]

Shang L, Hua H, Foo K, Martinez H, Watanabe K, Zimmer M, Kahler DJ, Freeby M, Chung W, LeDuc C, et al. beta-cell dysfunction due to increased ER stress in a stem cell model of Wolfram syndrome. Diabetes. 2014; 63:923–933. [PubMed: 24227685]

Shimomura K, Girard CA, Proks P, Nazim J, Lippiat JD, Cerutti F, Lorini R, Ellard S, Hattersley AT, Barbetti F, et al. Mutations at the same residue (R50) of Kir6.2 (KCNJ11) that cause neonatal diabetes produce different functional effects. Diabetes. 2006; 55:1705–1712. [PubMed: 16731833]

Steinthorsdottir V, Thorleifsson G, Reynisdottir I, Benediktsson R, Jonsdottir T, Walters GB, Styrkarsdottir U, Gretarsdottir S, Emilsson V, Ghosh S, et al. A variant in CDKAL1 influences insulin response and risk of type 2 diabetes. Nature genetics. 2007; 39:770–775. [PubMed: 17460697]

Unoki H, Takahashi A, Kawaguchi T, Hara K, Horikoshi M, Andersen G, Ng DP, Holmkvist J, Borch-Johnsen K, Jorgensen T, et al. SNPs in KCNQ1 are associated with susceptibility to type 2 diabetes in East Asian and European populations. Nature genetics. 2008; 40:1098–1102. [PubMed: 18711366]

Wei FY, Suzuki T, Watanabe S, Kimura S, Kaitsuka T, Fujimura A, Matsui H, Atta M, Michiue H, Fontecave M, et al. Deficit of tRNA(Lys) modification by Cdkal1 causes the development of type 2 diabetes in mice. The Journal of clinical investigation. 2011; 121:3598–3608. [PubMed: 21841312]

Yamagata K, Senokuchi T, Lu M, Takemoto M, Fazlul Karim M, Go C, Sato Y, Hatta M, Yoshizawa T, Araki E, et al. Voltage-gated K+ channel KCNQ1 regulates insulin secretion in MIN6 beta-cell line. Biochemical and biophysical research communications. 2011; 407:620–625. [PubMed: 21426901]

Yasuda K, Miyake K, Horikawa Y, Hara K, Osawa H, Furuta H, Hirota Y, Mori H, Jonsson A, Sato Y, et al. Variants in KCNQ1 are associated with susceptibility to type 2 diabetes mellitus. Nature genetics. 2008; 40:1092–1097. [PubMed: 18711367]

Zhang S, Liu J, MacGibbon G, Dragunow M, Cooper GJ. Increased expression and activation of c-Jun contributes to human amylin-induced apoptosis in pancreatic islet beta-cells. Journal of molecular biology. 2002; 324:271–285. [PubMed: 12441106]

Highlights

- An isogenic hESC-based platform to define precise roles of T2D associated genes.
- *CDKAL1*$^{-/-}$, *KCNJ11*$^{-/-}$, *KCNQ1*$^{-/-}$ beta-like cells show defective insulin secretion.
- *CDKAL1*$^{-/-}$ beta-like cells are hypersensitive to glucotoxcity and lipotoxicity;
- T5224 rescues *CDKAL1*$^{-/-}$ induced beta cell defects by inhibiting the *FOS/JUN* pathway.

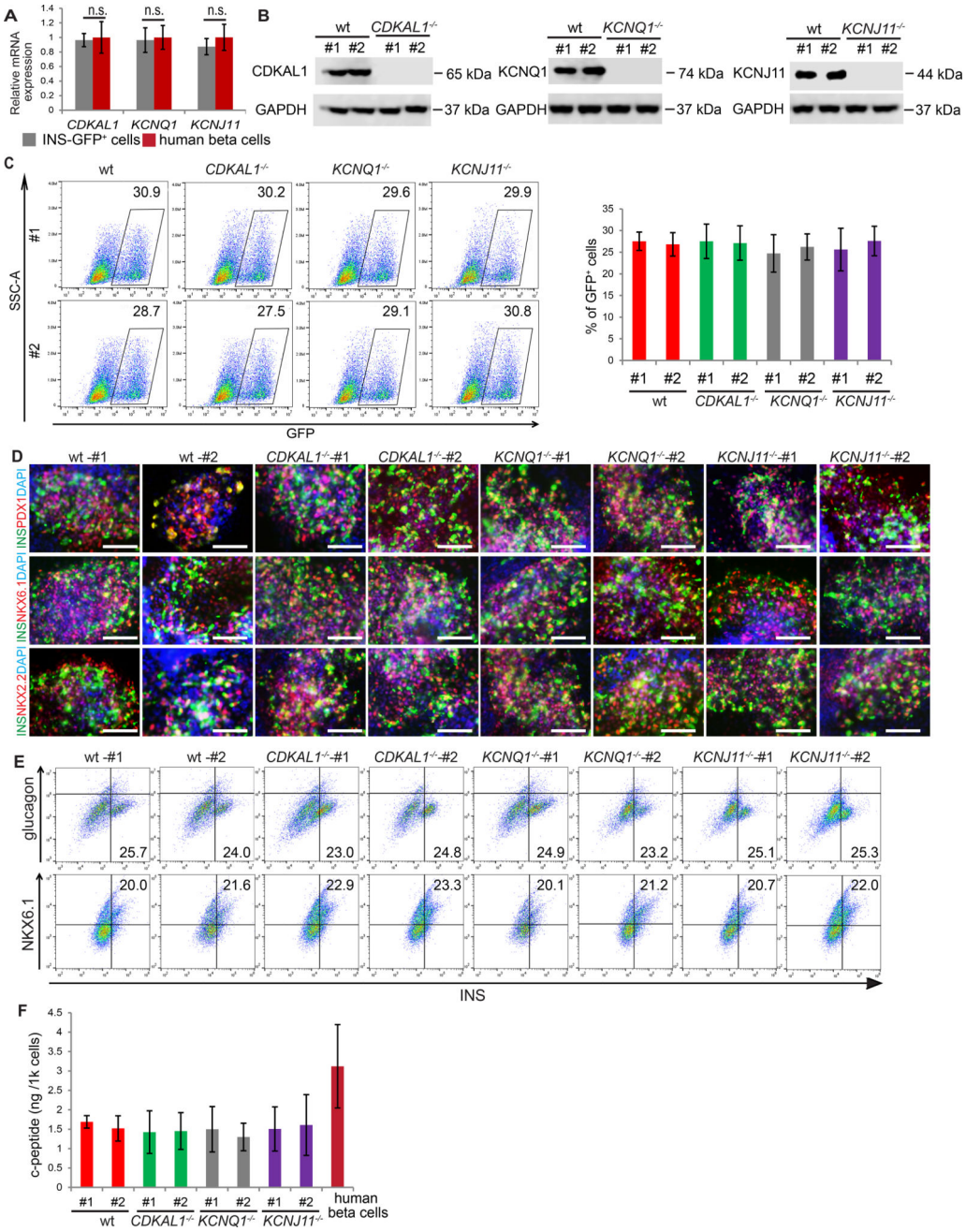

Figure 1. Biallelic mutation of *CDKAL1, KCNQ1* or *KCNJ11* does not affect differentiation or the expression of mature pancreatic beta cell markers

(A) qRT-PCR experiments confirmed the expression of *CDKAL1, KCNQ1*, and *KCNJ11* in insulin-GFP^{+} (INS-GFP^{+}) cells derived from INS$^{GFP/W}$ HES3 cells (n=4 independent experiments, error bars indicate S.D.) The expression level of *CDKAL1, KCNQ1*, and *KCNJ11* transcripts in primary human beta cells was calculated by dividing the expression level in primary human islets by the percentage of insulin^{+} cells. (B) Western blotting analysis of wildtype (wt) and isogenic mutant hESC-derived D30 cells. (C) Representative flow cytometry analysis and quantification of wt and isogenic mutant hESC-derived cells at day 30, n=3. (D) Immunocytochemistry analysis of wt and isogenic mutant hESC-derived

D30 cells. The insulin$^+$ cells express mature beta cell markers, including PDX1, NKX6.1 and NKX2.2. **S**cale bar = 100 μm. (E) Intracellular FACS analysis of D30 cells. (F) Total c-peptide content per 1 k insulin-GFP$^+$ cells as measured by ELISA, n=3. Total c-peptide content in primary human beta cells was calculated by dividing the total c-peptide in primary human islets by the percentage of insulin$^+$ cells. Clone #1 and #2 are two independent isogenic hESC clones carrying different frameshift mutations. hESCs were differentiated using protocol 2. The data is presented as mean±S.D. *p* values calculated by unpaired two-tailed Student's t-test were *p<0.05, **p<0.01, ***p<0.001. See also Figure S1.

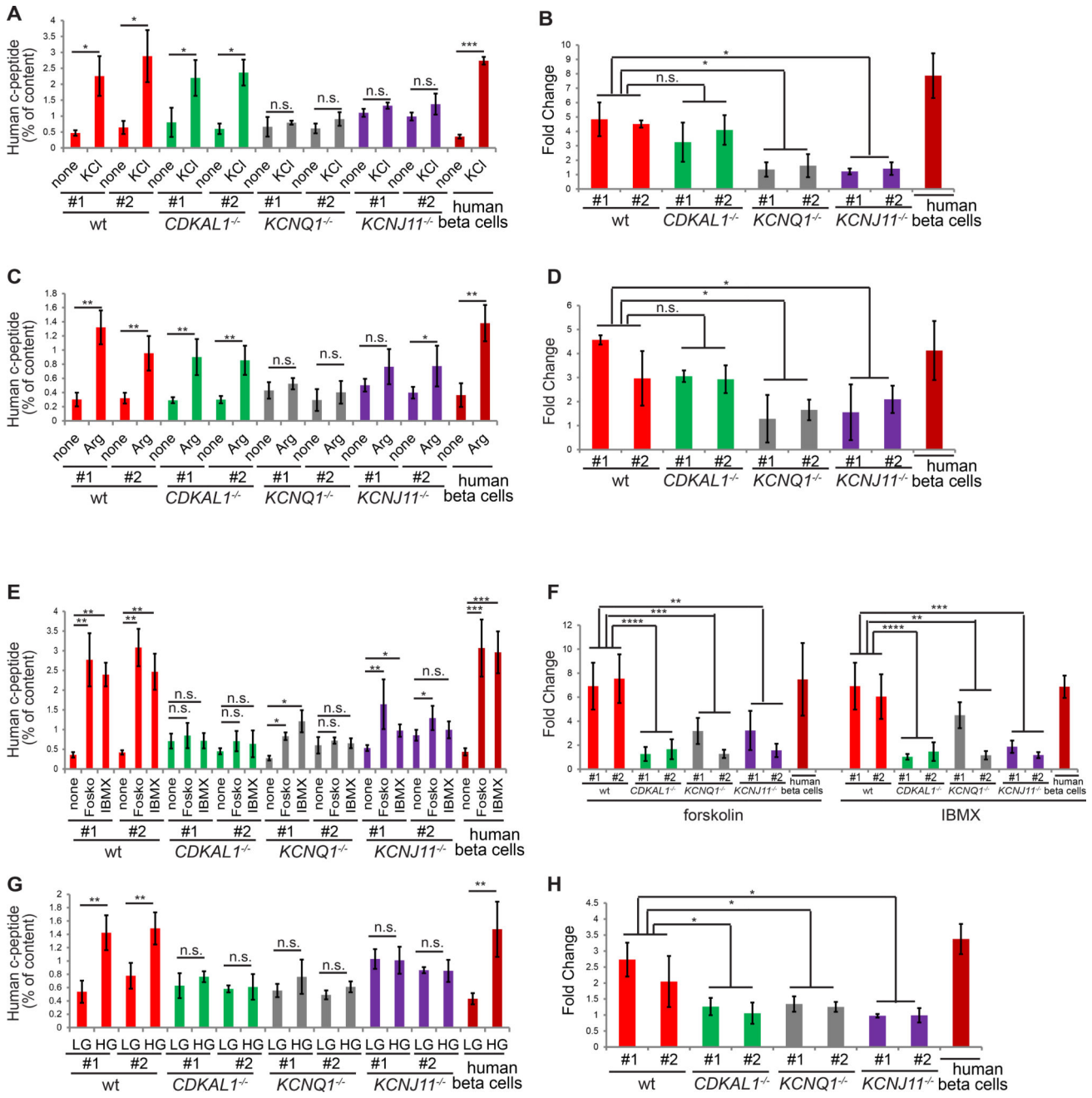

Figure 2. Biallelic mutation of *CDKAL1*, *KCNQ1* or *KCNJ11* impairs insulin secretion upon various stimulations

(A and B) Human c-peptide (% of content) (A) and fold change (B) of wildtype (wt) and isogenic mutant cells at day 30 with or without 30 mM KCl stimulation in the presence of 2 mM D-glucose, n=3. (C and D) Human c-peptide (% of content) (C) and fold change (D) of wildtype and isogenic mutant cells at day 30 with and without 10 mM arginine stimulation in the presence of 2 mM D-glucose, n=3. (E and F) Human c-peptide (% of content) (E) and fold change (F) of wildtype and isogenic mutant cells at day 30 with or without 20 μM forskolin and 50 μM IBMX stimulation in the presence of 2 mM D-glucose, n=3. (G and H) Human c-peptide (% of content) (G) and fold change (H) of wildtype and isogenic mutant

cells at day 30 with 2 mM or 20 mM D-glucose, n=3. Arg: arginine; forsk: forskolin; LG: 2 mM D-glucose; HG: 20 mM D-glucose. Human c-peptide secretion was calculated by dividing the secreted c-peptide by the total c-peptide of insulin-GFP^{+} cells or primary human beta cells. Clones #1 and #2 are two independent isogenic hESC clones carrying different frameshift mutations. hESCs were differentiated using protocol 2. The data is presented as mean±S.D. n.s. indicates a non-significant difference. *p* values calculated by unpaired two-tailed Student's t-test were *p<0.05, **p<0.01, ***p <0.001, ****p <0.0001. See also Figure S2.

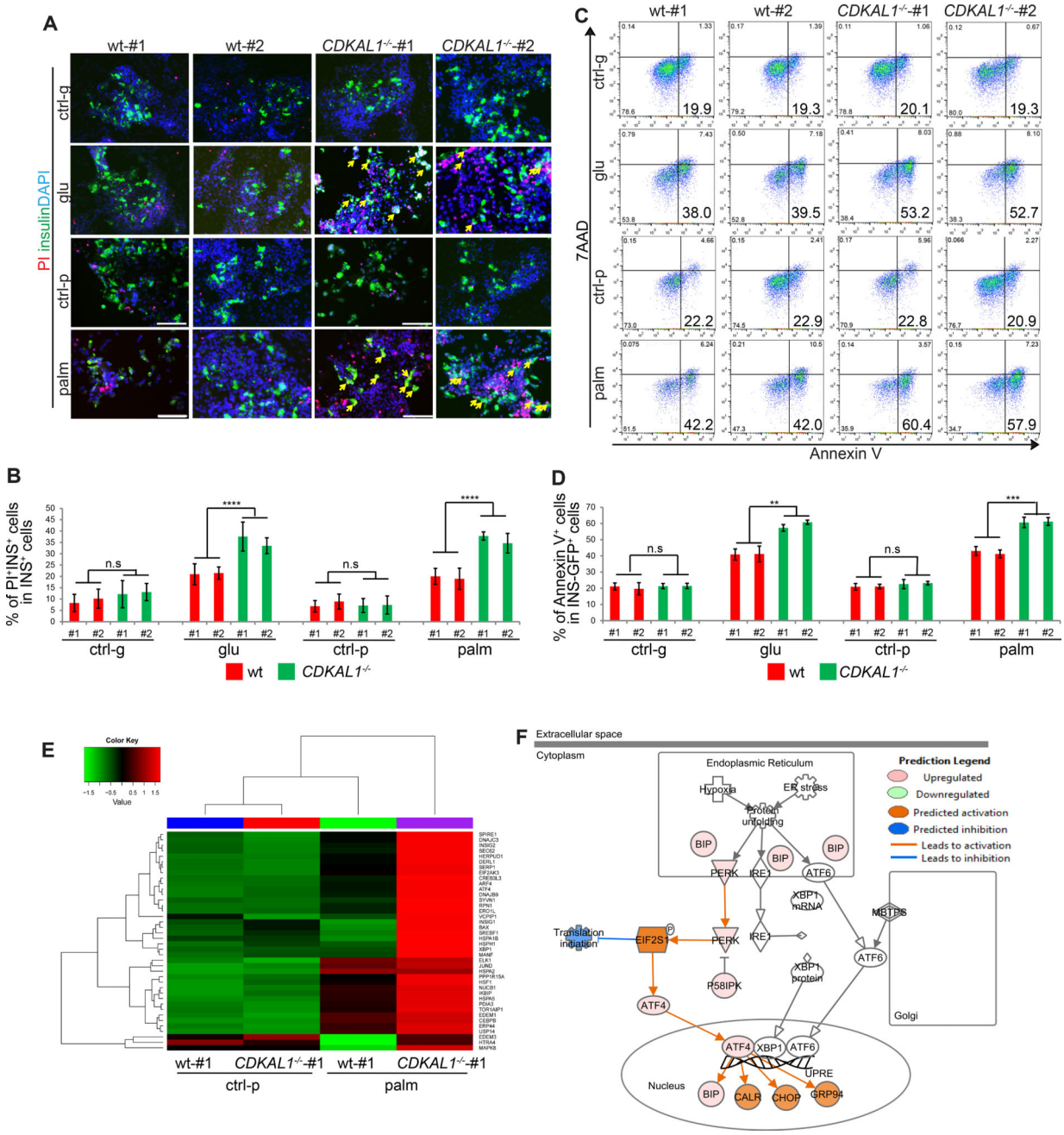

Figure 3. *CDKAL1*$^{-/-}$ insulin-GFP^{+} cells are hypersensitive to glucotoxicity and lipotoxicity

(A and B) Immunocytochemistry analysis (A) and quantification of the percentage (B) of PI^{+}/insulin^{+} cells in wildtype (wt) or *CDKAL1*$^{-/-}$ insulin^{+} cells cultured in the presence of 2 mM D-Glucose (ctrl-g), 35 mM D-Glucose (glu), no palmitate (ctrl-p) or 1 mM palmitate (palm). PI^{+}/insulin^{+} cells are highlighted by arrows. (C and D) Flow cytometry analysis (C) and quantification of the percentage (D) of Annexin V^{+} cells in wildtype and *CDKAL1*$^{-/-}$ insulin-GFP^{+} cells cultured as in (A). (E) Heat map representing the expression profiles of ER-stress related genes comparing wildtype and *CDKAL1*$^{-/-}$ insulin^{+} cells cultured in the absence or presence of 1 mM palmitate. (F) Ingenuity Pathway Analysis of genes that are >2

fold upregulated in *CDKAL1*$^{-/-}$ insulin^{+} cells cultured in the presence of 1 mM palmitate. INS: insulin; PI: propidium iodide. n=3 independent biological replicates. n.s. indicates a non-significant difference. Clone #1 and #2 are two independent isogenic hESC clones carrying different frameshift mutations. hESCs were differentiated using protocol 2. *p* values calculated by unpaired two-tailed Student's t-test were **p*<0.05, ***p*<0.01, ****p*<0.001, *****p*<0.0001. Scale bar = 100 μm. See also Figure S3.

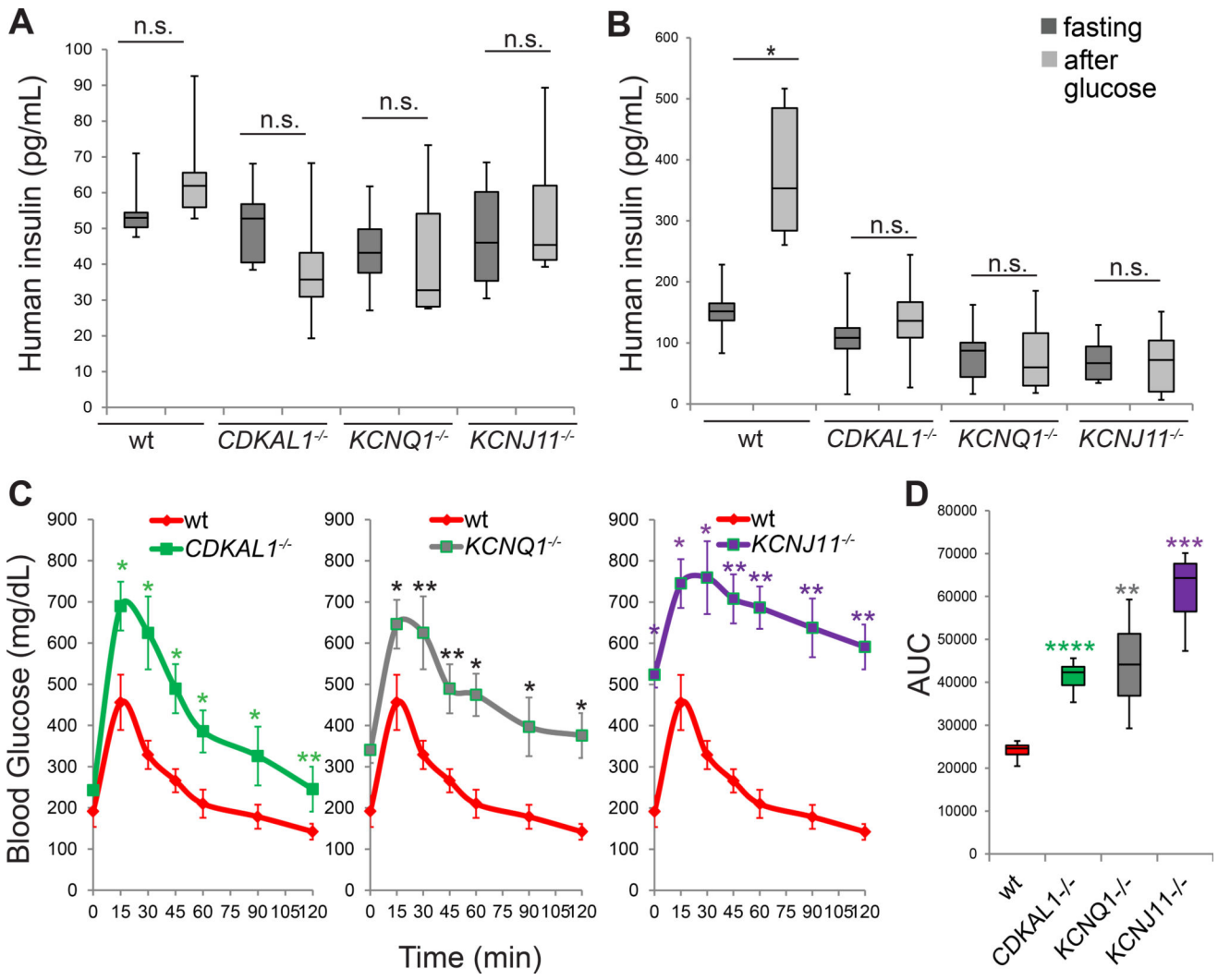

Figure 4. *CDKAL1*$^{-/-}$, *KCNQ1*$^{-/-}$ and *KCNJ11*$^{-/-}$ cells show defective glucose stimulated insulin secretion and impaired ability to maintain glucose homeostasis after transplantation into streptozotocin-treated immunodeficient mice

(A) human insulin GSIS at 2 weeks after transplantation of the mutant cells compared to wildtype cells (wt). (B) GSIS secretion of SCID-beige mice carrying human cells at 6 weeks after transplantation. *p* values calculated by one-way repeated measures ANOVA. (C and D) Intraperitoneal glucose tolerance test (IPGTT) (C) and area under the curve (AUC) (D) of STZ treated mice 6 weeks after transplantation. *p* values calculated by two-way repeated measures ANOVA with a Bonferroni test for multiple comparisons between wt and mutant cells. n=8 mice for each condition. hESCs were differentiated using protocol 2. n.s. indicates a non-significant difference. *p* values were *p<0.05 and ** p<0.01, *** p<0.001, **** p<0.0001. See also Figure S4.

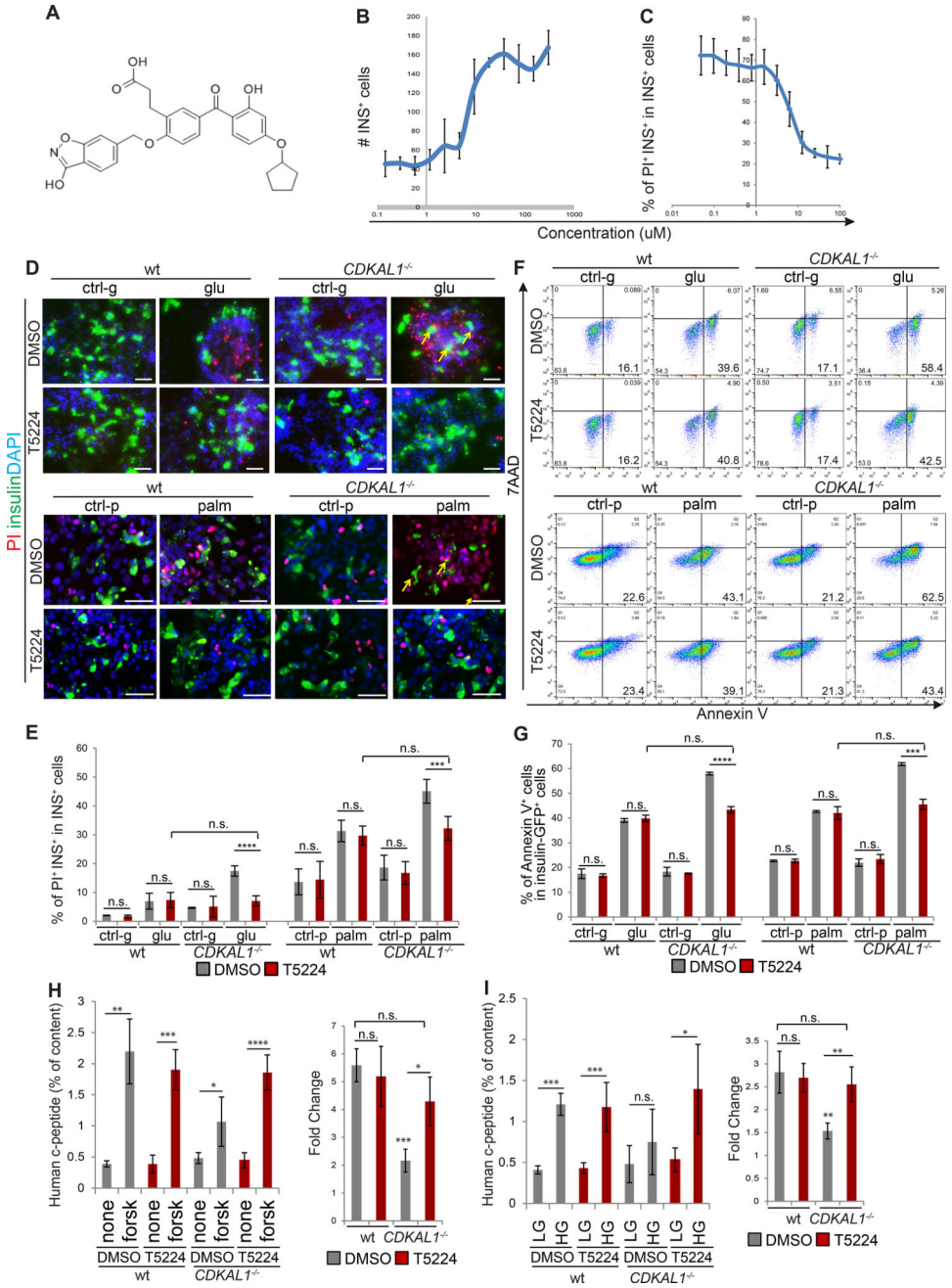

Figure 5. A high content chemical screen identifies a drug candidate that rescues glucolipotoxicity caused specifically by mutations in *CDKAL1*

(A) Chemical structure of T5224. (B and C) Efficacy curve of T5224 on the number of insulin$^+$ cells (B) and the percentage of PI$^+$INS$^+$ cells (C). PI: propidium iodide. (D and E) Immunocytochemistry analysis (D) and quantification of the percentage (E) of PI$^+$/insulin$^+$ cells in wildtype (wt) and *CDKAL1*$^{-/-}$, insulin$^+$ cells treated with 30 μM T5224 when cultured in the presence of 2 mM D-Glucose (ctrl-g), 35 mM D-Glucose (glu), no palmitate (ctrl-p) or 1 mM palmitate (palm). PI$^+$/insulin$^+$ cells are highlighted by arrows. (F and G) Flow cytometry analysis (F) and quantification (G) of apoptotic rate for wt or *CDKAL1*$^{-/-}$ insulin-GFP$^+$ cells treated with DMSO or T5224. (H and I) T5224 also rescues the impaired

forskolin-induced (H) and glucose-induced insulin secretion (I). Experiments in Figure 5A–C were performed using cells derived from protocol 1. Experiments in Figure 5D–I were performed using cells derived from protocol 2. n=3 independent biological replicates for each condition. n.s. indicates a non-significant difference. *p* values calculated by unpaired two-tailed Student's t-test were *$p<0.05$, **$p<0.01$, ***$p<0.001$, ****$p<0.0001$. Scale bar = 50 μm. See also Figure S5.

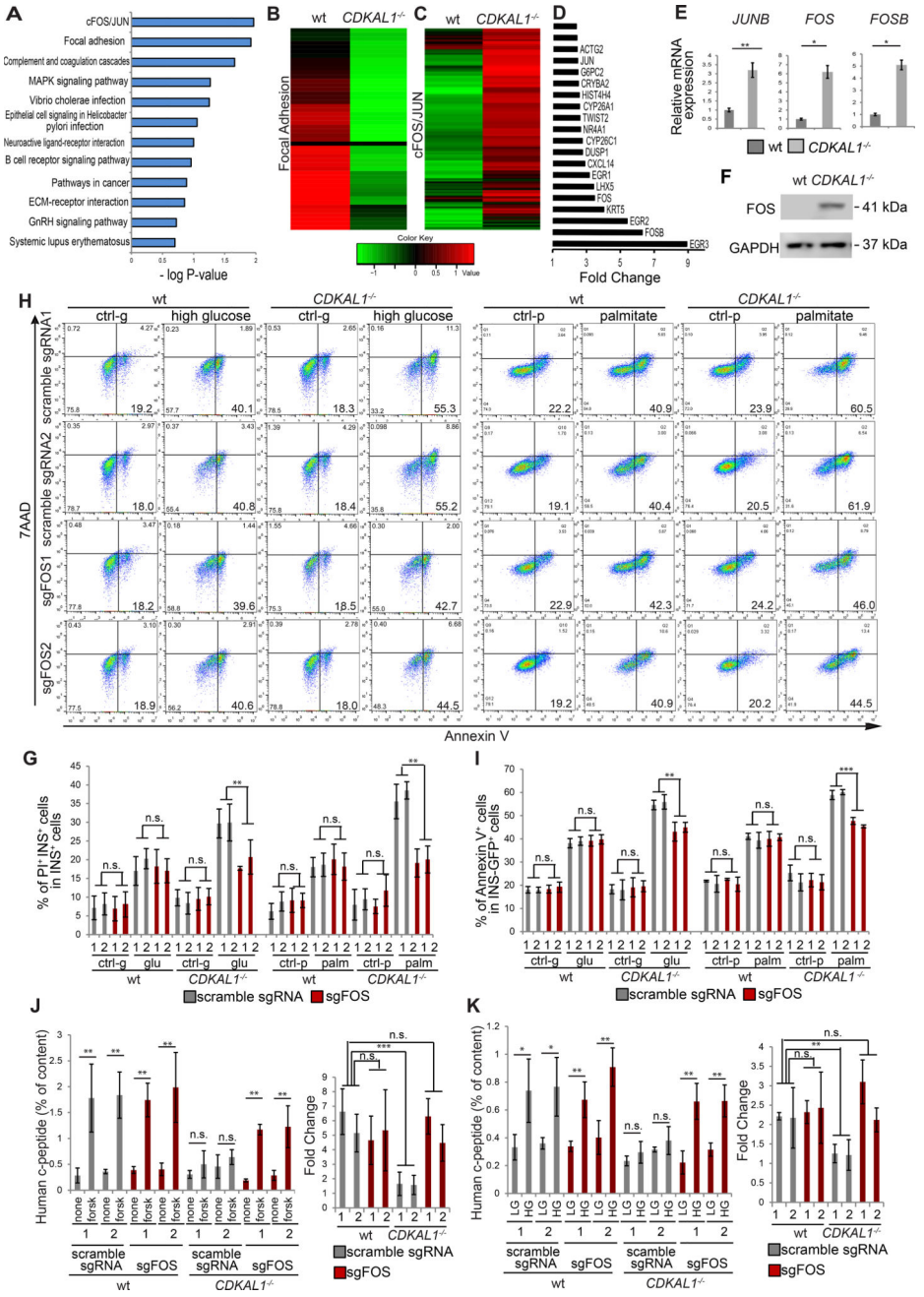

Figure 6. T5224 rescues beta cell defects caused by *CDKAL1* mutation through inhibiting the *FOS/JUN* pathway

(A) Pathway enrichment analysis on up/down-regulated genes in *CDKAL1*$^{-/-}$ insulin-GFP^{+} cells using the DAVID function annotation tool. (B) Heat map of *Focal Adhesion* pathway associated genes comparing wildtype (wt) and *CDKAL1*$^{-/-}$ insulin-GFP^{+} cells. (C) Heat map of *FOS/JUN* pathway associated genes comparing wt and *CDKAL1*$^{-/-}$ insulin-GFP^{+} cells. (D) Top 20 upregulated genes in *CDKAL1*$^{-/-}$ insulin-GFP^{+} cells as compared to wildtype cells. (E) qRT-PCR analysis of *JUNB, FOS, FOSB* expression in wildtype and *CDKAL1*$^{-/-}$ insulin-GFP^{+} cells. (F) Western blotting analysis of FOS protein in wildtype and *CDKAL1*$^{-/-}$ cells at D30 of differentiation. (G) Targeted mutation of *FOS* rescues the

high death rate in *CDKAL1*$^{-/-}$ insulin-GFP^{+} cells in the presence of 35 mM D-glucose or 1 mM palmitate. (H and I) Flow cytometry analysis (H) and quantification of apoptotic rate (I) of *CDKAL1*$^{-/-}$ insulin-GFP^{+} cells expressing Cas9 and either scrambled sgRNA or sgFOS. (J and K) Mutation of *FOS* rescues the impaired forskolin-induced (J) and glucose-induced (K) insulin secretion that is caused by mutation of *CDKAL1*. SgFOS 1# and 2# represent two independent sgRNAs targeting different locations of exon1 of *c-FOS*. Scramble sgRNA #1 and Scramble #2 "target" controls were designed to have low homology to the human genome and are used as non-targeting controls. hESCs were differentiated using protocol 2. The data is presented as mean±S.D. n.s. indicates a non-significant difference. *p* values calculated by unpaired two-tailed Student's t-test were *p<0.05, **p<0.01, ***p<0.001. See also Figure S6.

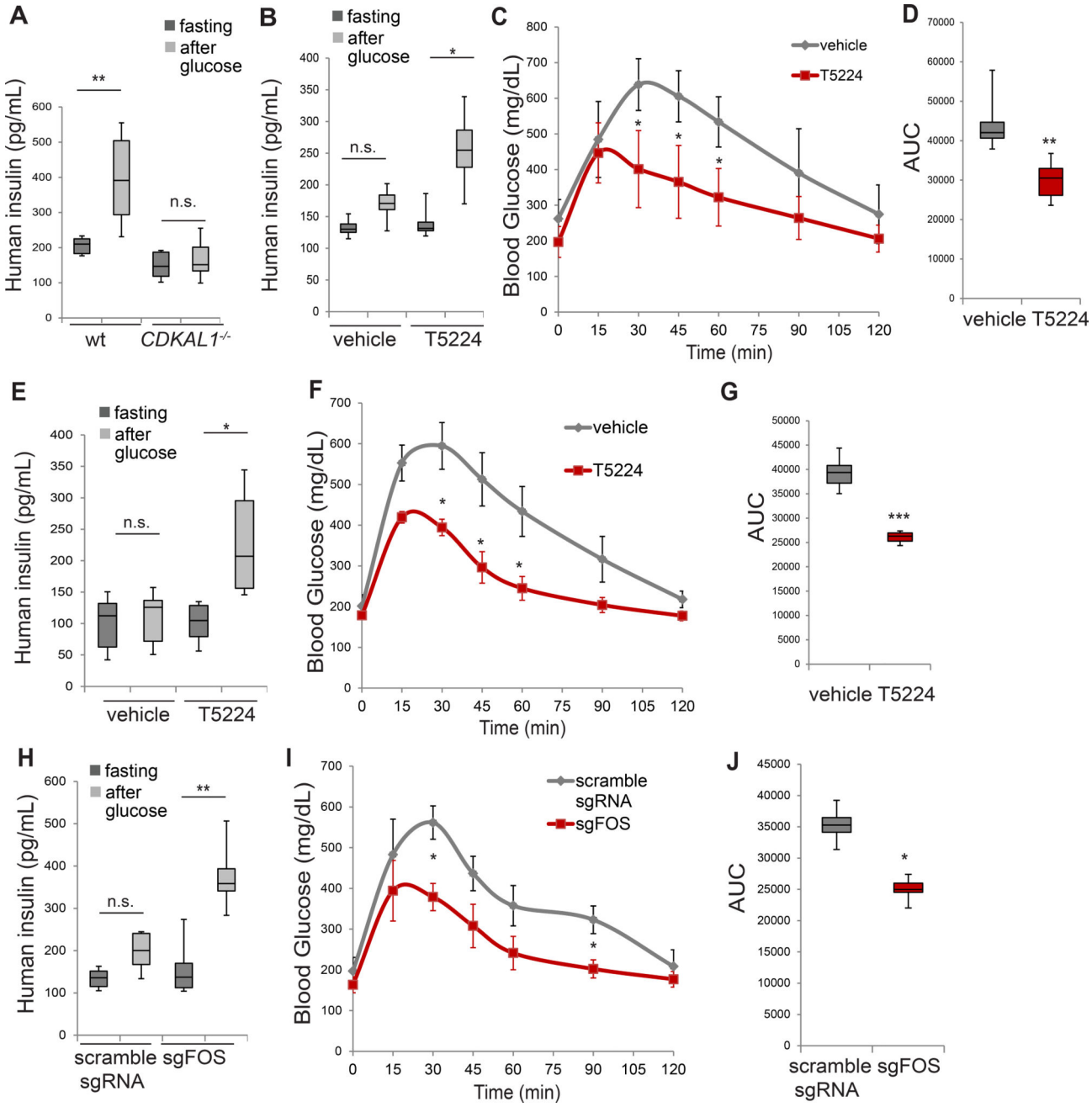

Figure 7. T5224 or loss of *FOS* rescues the function of *CDKAL1*$^{-/-}$ cells in SCID-beige mice carrying human cells

(A) Human insulin GSIS at 10 weeks after transplantation of mutant cells compared to wildtype cells (wt). (B) GSIS secretion of SCID-beige mice carrying human cells after glucose stimulation 48 hours after treatment with 300 mg/kg T5224 or vehicle. (C and D) IPGTT (C) and AUC (D) of mice transplanted with *CDKAL1*$^{-/-}$ cells treated with 300 mg/kg T5224 or vehicle. (E) GSIS secretion of SCID-beige mice carrying human cells after glucose stimulation after treatment with T5224 or vehicle twice a week for four weeks. (F and G) IPGTT (F) and AUC (G) of mice transplanted with *CDKAL1*$^{-/-}$ cells treated with 300 mg/kg T5224 or vehicle twice a week for 4 weeks. (H) GSIS secretion of SCID-beige

mice transplanted with *CDKAL1*$^{-/-}$ cells carrying scramble sgRNA or *CDKAL1*$^{-/-}$ cells carrying sgFOS. (I and J) IPGTT (I) and AUC (J) of mice transplanted with *CDKAL1*$^{-/-}$ cells carrying scramble sgRNA or *CDKAL1*$^{-/-}$ cells carrying sgFOS at 6 weeks after transplantation. n=8 mice for each condition. hESCs were differentiated using protocol 2. In GSIS assay, *p* values were calculated by one-way repeated measures ANOVA. In IPGTT assay, *p* values were calculated by two-way repeated measures ANOVA with a Bonferroni test for multiple comparisons between DMSO and T5224 treated conditions. *p* values were **p*<0.05, ** *p*<0.01, ****p*<0.001. See also Figure S7.